Molecular hydrogen in silicon: A path-integral simulation

Carlos P. Herrero and Rafael Ramírez
Instituto de Ciencia de Materiales, Consejo Superior de Investigaciones Científicas (CSIC), Campus de Cantoblanco, 28049 Madrid, Spain

(Received 4 May 2009; revised manuscript received 29 June 2009; published 29 July 2009)

Molecular hydrogen in silicon has been studied by path-integral molecular-dynamics simulations in the canonical ensemble. Finite-temperature properties of these point defects were analyzed in the range from 300 to 900 K. Interatomic interactions were modeled by a tight-binding potential fitted to density-functional calculations. The most stable position for these impurities is found at the interstitial *T* site with the hydrogen molecule rotating freely in the Si cage. Vibrational frequencies have been obtained from a linear-response approach, based on correlations of atom displacements at finite temperatures. The results show a large anharmonic effect in the stretching vibration, ω_s, which is softened with respect to a harmonic approximation by about 300 cm^{-1}. The coupling between rotation and vibration causes an important decrease in ω_s for rising temperature.

DOI: 10.1103/PhysRevB.80.035207 PACS number(s): 61.72.uf, 61.72.jj, 63.20.Pw, 71.15.Pd

I. INTRODUCTION

Hydrogen can be incorporated into semiconductors both intentionally and unintentionally during manufacturing processes carried out for technological applications. It appears in these solids in a number of different configurations: as an isolated interstitial, bound to impurities, bound to native defects, in molecular form, etc.[1–3] In the early 1980s, isolated hydrogen molecules were predicted to be stable in crystalline semiconductors and to play an important role in the diffusion of hydrogen in these materials.[4,5] However, they were not unambiguously detected by spectroscopic methods until more than ten years later.[6–8]

Vibrational transitions have been reported for interstitial H_2 in Si,[7,8] Ge,[9] and GaAs.[6] In these semiconductors, theory predicts that the H_2 molecule is stable at an interstitial tetrahedral (*T*) site and behaves as a nearly free rotator.[10,11] This gives rise at low temperatures to two stretching local vibrational modes originating from para and ortho nuclear states, which are split due to rovibrational coupling.[12]

Here we will concentrate on isolated hydrogen molecules in the bulk of crystalline silicon. The interest of this problem is twofold. On one side, it is important as a point defect in semiconductor physics, for its relevance in the hydrogen diffusion and stability in these materials. On the other side, from a fundamental point of view, H_2 in silicon is an example of a light molecule sitting and moving in a confined geometry, and one can study its behavior when localized in a spatial region with extension of a few Å.

Earlier theoretical studies of molecular hydrogen in semiconductors have concentrated on determining the lowest-energy site and stretching frequency of the molecule, including in some cases anharmonic effects derived from the calculated potential-energy surface[10,11,13–15] as well as the quantum rotation of H_2 molecules.[16,17] Density-functional electronic-structure calculations in condensed matter are very reliable, but they treat atomic nuclei as classical particles, and typical quantum effects like zero-point vibrations are not directly accessible. These effects can be included by employing harmonic or quasiharmonic approximations, but are difficult to take into account when large anharmonicities are present, as can happen for light impurities like hydrogen.

To consider the quantum character of the nuclei, the path-integral molecular dynamics (or Monte Carlo) approach has proved to be very useful. A remarkable advantage of this method is that all nuclear degrees of freedom can be quantized in an efficient manner, thus including both quantum and thermal fluctuations in many-body systems at finite temperatures. In this way, Monte Carlo or molecular-dynamics sampling applied to evaluate finite-temperature path integrals allows one to carry out quantitative and nonperturbative studies of highly anharmonic effects in solids.[18,19]

In this paper, the path-integral molecular-dynamics (PIMD) method is used to study interstitial hydrogen molecules in silicon. Special attention has been paid to the vibrational properties of these impurities, by considering anharmonic effects on their quantum dynamics and the rovibrational coupling at different temperatures. The results of the present calculations show that anharmonic effects lead to a significant decrease of the vibrational frequencies of the impurities, as compared to a harmonic approximation. We have analyzed the isotopic effect on structural and vibrational properties of these molecules, by considering also molecular deuterium (D_2). Path-integral methods analogous to that employed in this work have been applied earlier to study hydrogen in metals[18] and semiconductors[20–24] as well as on surfaces.[25,26] In connection with the behavior of molecular hydrogen in confined regions H_2 has been studied inside carbon nanotubes by diffusion Monte Carlo.[27] Also, path-integral simulation methods have been extensively applied to study condensed phases of hydrogen in molecular form.[28–31]

The paper is organized as follows. In Sec. II, we describe the computational method and the models employed in our calculations. Our results are presented in Sec. III, dealing with the kinetic energy of the molecules, spatial delocalization, interatomic distance, and vibrational frequencies. Sec. IV includes a discussion of the results and a summary.

II. COMPUTATIONAL METHOD

A. Path-integral molecular dynamics

In the path-integral formulation of statistical mechanics employed here, the partition function is evaluated by a dis-

cretization of the density matrix along cyclic paths, consisting of a finite number P (Trotter number) of "imaginary-time" steps.[32,33] In the implementation in numerical simulations, this discretization gives rise to the appearance of P "beads" for each quantum particle. These beads can be formally treated as classical particles so that the partition function of the original quantum system is isomorph to that of a classical one. This isomorphism is obtained by replacing each quantum particle by a ring polymer consisting of P classical particles connected by harmonic springs.[18,19] In many-body problems, the configuration space is usually sampled by Monte Carlo or molecular-dynamics techniques. Here, we have employed the PIMD method which has been found to need less computer time for the present problem. We have used effective algorithms for performing PIMD simulations in the canonical NVT ensemble, as those described in detail by Martyna *et al.*[34] and Tuckerman.[35]

Our calculations have been performed within the adiabatic (Born-Oppenheimer) approximation, which allows one to define a potential-energy surface for the nuclear motion. An important issue in this kind of simulations is the proper description of interatomic interactions, which should be as realistic as possible. Since using true density-functional (DF) or Hartree-Fock-type calculations requires computer resources that would restrict enormously the size of our simulation cell, we obtain the Born-Oppenheimer surface from a tight-binding (TB) effective Hamiltonian, derived from DF calculations.[36] The TB energy consists of two parts, the first one is the sum of energies of occupied one-electron states, and the second one is given by a pairwise repulsive interatomic potential.[36] For the present study the H–H pair potential was tuned to reproduce the main features of known effective interatomic potentials, such as the Morse potential.[37] The capability of TB methods to simulate different properties of solids and molecules has been reviewed by Goringe *et al.*[38] The convergence of the total energy with the sampling in reciprocal space was checked by using several sets of special k points.[39] We found that a set of 4 k points provides already good convergence (relative error less than 0.001% in the total energy). The use of only the Γ point introduces a small systematic error in the total energy that affects slightly the value of energy differences between different spacial configurations of H_2 in silicon with typical errors of about 0.01 eV. These results justify that the simulations presented in this work were performed by using only the Γ point for the reciprocal space sampling.

Simulations were carried out on a $2\times2\times2$ supercell of the silicon face-centered cubic cell with periodic boundary conditions, containing 64 Si atoms and a hydrogen (or deuterium) molecule. For comparison, we also carried out simulations of pure silicon, using the same supercell size. Sampling of the configuration space has been carried out at temperatures between 300 and 900 K. The electronic-structure calculations were performed without considering a temperature-dependent Fermi filling of the electronic states, which is reasonable for this temperature range. For a given temperature, a typical simulation run consisted of 10^4 PIMD steps for system equilibration, followed by 5×10^5 steps for the calculation of ensemble-average properties. To keep a nearly constant precision in the path-integral results at different temperatures, we have employed a Trotter number that scales as the inverse temperature. In particular, we have taken $PT=18000$ K, which means $P=60$ for $T=300$ K. Quantum exchange effects between protons or deuterons were not considered, as they are negligible at the temperatures considered here, so that both atomic nuclei in a molecule were treated as if they were distinguishable particles.

The simulations were carried out by employing a staging transformation for the bead coordinates. The canonical ensemble was generated by coupling chains of four Nosé-Hoover thermostats (with mass $Q=\beta\hbar^2/5P$) to each degree of freedom.[40] To integrate the equations of motion, we used a reversible reference-system propagator algorithm, which allows one to define different time steps for the integration of fast and slow degrees of freedom.[34] The time step Δt associated to the calculation of DF-TB forces was taken in the range between 0.1 and 0.4 fs, which was found to be appropriate for the interactions, atomic masses, and temperatures under consideration. For the evolution of the fast dynamical variables, including the thermostats and harmonic bead interactions, we used a smaller time step $\delta t=\Delta t/4$. We note that for H_2 in silicon at 300 K, a simulation run consisting of 5×10^5 PIMD steps needs the calculation of forces and energy with the TB code for 3×10^7 configurations, which has required the use of parallel computers.

B. Calculation of anharmonic vibrational frequencies

Vibrational frequencies of impurities in solids are important characteristics, which depend on the site that they actually occupy and on its interactions with the nearby hosts atoms. In this context, the question arises whether the oscillator frequencies associated to an impurity can be extracted by assuming the host atoms fixed in the relaxed geometry corresponding to the minimum-energy configuration. This is a method usually employed to calculate vibrational frequencies of impurities in crystals. On the other side, when the host atoms are allowed to relax by following the impurity motion, the potential-energy surface is flatter than when the host atoms are fixed. To obtain an approach for the actual vibrational frequencies of the impurities, one can calculate the eigenvalues of the dynamical matrix of the whole simulation cell, and obtain the frequencies in the harmonic approximation (HA). However, for light impurities the anharmonicity can be appreciable and the harmonic frequencies are only a first (maybe crude) approximation.

To calculate anharmonic frequencies we will use here a method based on the linear response (LR) of the system to vanishingly small forces applied on the atomic nuclei. To this end, we consider a LR function, the static isothermal susceptibility χ^T, that is readily derived from PIMD simulations of the equilibrium solid, without dealing explicitly with any external forces in the simulation. This approach represents a significant improvement as compared to a standard harmonic approximation.[37] The tensor χ^T allows one to derive a LR approximation to the low-lying excitation energies of the vibrational system that is applicable even to highly anharmonic situations. For a system with $3N$ vibrational degrees of freedom, the LR approximation for the frequencies reads

$$\omega_n = \frac{1}{\sqrt{\delta_n}}, \tag{1}$$

where $\delta_n (n=1,\ldots,3N)$ are eigenvalues of χ^T, and the LR approximation to the low-lying excitation energy of vibrational mode n is given by $\hbar\omega_n$. Details on the method and illustrations of its ability for predicting vibrational frequencies of solids and molecules are given elsewhere.[37,41–43]

III. RESULTS

A. Minimum-energy configuration

We first present results for classical calculations at zero temperature, where the atoms are treated as pointlike particles without spatial delocalization. The employed interatomic potential gives reliable results for molecular hydrogen *in vacuo*. The lowest-energy molecular configuration corresponds to a distance R_0 between hydrogen atoms of 0.741 Å. At this distance we obtain for H_2 in a harmonic approximation a stretching frequency of 4397 cm^{-1}.

For H_2 as an impurity in silicon, we find a lowest-energy position for the center of gravity of the molecule located at an interstitial T site. The minimum energy is found for the H–H axis along a ⟨100⟩ crystal direction, with a distance between H atoms of 0.752 Å. Moreover, changes in the energy for molecule rotation keeping its center of gravity at a T site are very small, in agreement with earlier calculations based on DF theory.[10,11,14] In silicon an increase in the H–H distance of about 0.01 Å was found with respect to the molecule in vacuo, as expected for an attractive interaction between each H and the nearby Si atoms.

Assuming the H_2 molecule at a T site, and oriented along the ⟨100⟩ direction, we find in the harmonic approximation a stretching frequency of 4071 cm^{-1}, close to the harmonic value of 4015 cm^{-1} derived from the (anharmonic) vibrational frequency observed in Raman spectra.[44] This represents a decrease in more than 300 cm^{-1} vs the harmonic frequency for the molecule in the gas phase, in line with a weakening of the H–H bond due to interaction with the silicon lattice, as discussed earlier.[10,11] In the HA we also find frequencies $\omega_{\parallel}=954$ cm^{-1} and $\omega_{\perp}=1385$ cm^{-1} (twofold degenerate) for motion of the molecule along and perpendicular to the H–H axis in the silicon cage. These two vibrational frequencies are not expected to be observable because they will be mixed by the free rotation of the molecule (see below).

B. Kinetic energy

We now turn to our PIMD simulations at finite temperatures. To obtain insight into the motion of H_2 around the tetrahedral site, we will consider various models in which the number of degrees of freedom will be successively increased. In particular, we will consider: (1) motion of the H_2 molecule in one dimension (along the H–H bond) in a fixed and unrelaxed silicon lattice; (2) free motion (in 3d) of the hydrogen molecule with fixed host atoms, and (3) free motion of H_2 with mobile Si atoms. In the latter case, all 66 atomic nuclei in the simulation cell are treated as quantum particles.

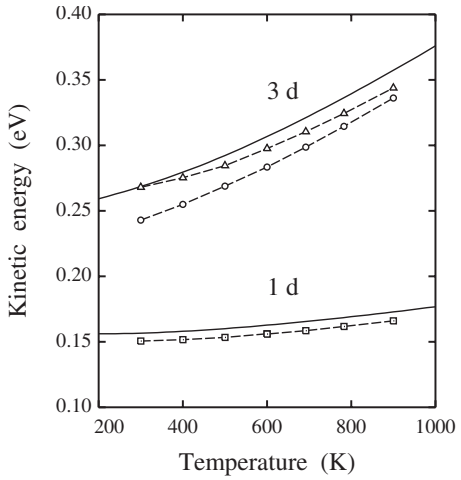

FIG. 1. Temperature dependence of the kinetic energy of molecular hydrogen in silicon for various approximations. Squares: motion of H_2 in one dimension with fixed host atoms; circles: free motion of H_2 in a fixed silicon lattice; triangles: free motion of H_2 with unrestricted motion of the Si atoms. Solid lines correspond to harmonic approximations for H_2 motion in one and three dimensions. Dashed lines are guides to the eye.

In our finite-temperature simulations for cases (2) and (3), where the molecule can rotate around the T site, we observe a free molecular rotation, without any preferential orientation. This is in agreement with earlier conclusions derived from theoretical[10,11] and experimental[45,12] works, and with the fact that the potential-energy surface for the rotation does not display deep minima.

In Fig. 1 we show the kinetic energy of the hydrogen molecule in the three considered approaches. Symbols indicate results derived from our PIMD simulations using the so-called virial estimator[46,40] and solid lines represent the kinetic energy expected in a harmonic approximation. For 1d motion of H_2 (approach 1, squares) we find a slight increase in E_k as temperature is raised. In this approach, results of the simulations are somewhat lower than those derived for the HA, as expected for a softening of the vibrations due to the anharmonicity of the interatomic potential. In fact, the linear-response method introduced in Sect. II B gives in this case for the stretching frequency $\omega_s=3770$ cm^{-1} at 300 K, which means a decrease in about 300 cm^{-1} with respect to the harmonic model for H_2 in silicon ($\omega_s=4071$ cm^{-1}).

Circles in Fig. 1 correspond to our approach 2 with H_2 moving in a fixed silicon lattice. Now we are dealing with six degrees of freedom, two of which correspond to molecular rotation. This approximation gives again values of the kinetic energy smaller than those predicted by the HA (solid line). This harmonic approximation includes a classical description of the two rotational degrees of freedom of the H_2 molecule. To analyze the kinetic energy of the defect complex in model 3 (all atoms are free to move), we calculate E_k for the simulation cell with and without the H_2 molecule: $E_k(\text{defect})=E_k(64\text{Si}+\text{H}_2)-E_k(64\ \text{Si})$. The results (triangles) lie appreciably above those obtained for model 2, indicating

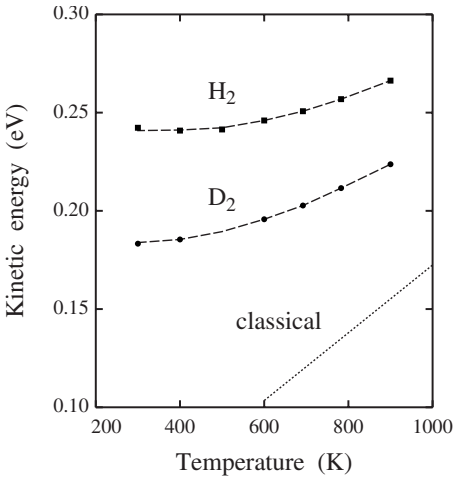

FIG. 2. Temperature dependence of the vibrational part of the kinetic energy of H_2 and D_2, as derived from approach 3 with free motion of all atoms in the simulation cell. Symbols indicate results derived from PIMD simulations: squares for H_2 and circles for D_2. Error bars are on the order of the symbol size. Dashed lines are guides to the eye. The dotted line corresponds to the classical limit with four degrees of freedom.

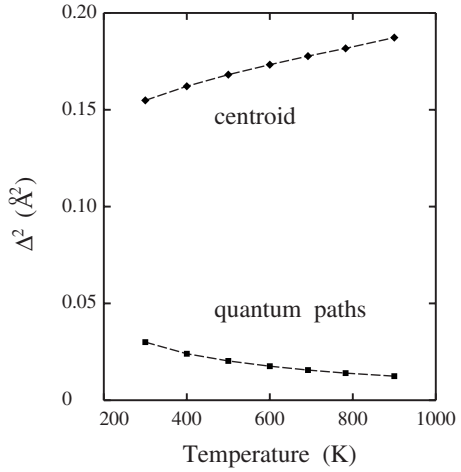

FIG. 3. Spatial delocalization of atomic nuclei (protons) in H_2. Diamonds indicate the mean-square displacement of the centroid of the quantum paths, Δ_C^2, and squares correspond to the mean-square radius of gyration of the paths, Δ_Q^2.

a non-negligible coupling in the motion of interstitial molecule and host atoms.

At the temperatures considered here, rotation of H_2 can be considered with a high precision to be classical. This means that its contribution to the kinetic energy of the molecule will be k_BT (two degrees of freedom). Then, we can subtract this classical energy from E_k derived from the PIMD simulations to obtain a vibrational contribution to the kinetic energy E_k^v. This part of the kinetic energy is shown in Fig. 2 for H_2 (squares) and D_2 (circles). At low temperature it converges to values close to 0.24 and 0.18 eV, respectively. This gives a ratio $E_k^v(H_2)/E_k^v(D_2)=1.33$, somewhat smaller than the limit 1.41 expected for harmonic vibrations at low temperatures. This deviation may be due to both anharmonicity in the interatomic interaction and changes in the effective mass caused by coupling to the host atoms. This ratio decreases as T is raised and amounts to 1.19 at 900 K. For comparison we also present in Fig. 2 the kinetic energy corresponding to the classical limit with four vibrational degrees of freedom ($2k_BT$, dotted line).

C. Atomic delocalization

To study the spatial delocalization of a quantum particle from PIMD simulations, it is convenient to consider the center of gravity (centroid) of the quantum paths of the particle, defined as

$$\bar{\mathbf{r}} = \frac{1}{P}\sum_{i=1}^{P} \mathbf{r}_i, \tag{2}$$

$\mathbf{r}_i$ being the coordinates of the "beads" in the associated ring polymer.

The mean-square displacement of a quantum particle along a PIMD simulation run is then given by

$$\Delta^2 = \frac{1}{P}\left\langle \sum_{i=1}^{P} (\mathbf{r}_i - \langle\bar{\mathbf{r}}\rangle)^2 \right\rangle, \tag{3}$$

where $\langle \ldots \rangle$ indicates a thermal average at temperature T. After some straightforward manipulations, one can write Δ^2 as

$$\Delta^2 = \Delta_Q^2 + \Delta_C^2, \tag{4}$$

with

$$\Delta_Q^2 = \frac{1}{P}\left\langle \sum_{i=1}^{P} (\mathbf{r}_i - \bar{\mathbf{r}})^2 \right\rangle \tag{5}$$

and

$$\Delta_C^2 = \langle (\bar{\mathbf{r}} - \langle\bar{\mathbf{r}}\rangle)^2 \rangle. \tag{6}$$

The first term, Δ_Q^2, is the mean-square "radius of gyration" of the ring polymers associated to the quantum particle (atomic nucleus) under consideration.[18] This is a measure of the average extension of the paths and, therefore, of the importance of quantum effects in a given problem. The second term in Eq. (4) is the mean-square displacement of the center of gravity of the paths. This term is the only one surviving at high temperatures since in the classical limit each path collapses onto a single point (hence with a vanishing radius of gyration). For situations in which the anharmonicity is not extremely large, the distribution of $\bar{\mathbf{r}}$ is similar to that of a classical particle in the same potential, and thus Δ_C^2 can be considered as a kind of semiclassical delocalization.

Going back to our problem of H_2 in silicon, for each hydrogen atom in the molecule we have calculated separately both terms giving the atomic delocalization in Eq. (4). Shown in Fig. 3 are the values of Δ_Q^2 (spreading of the quantum paths, squares) and Δ_C^2 (centroid delocalization, diamonds), as derived from our PIMD simulations at several temperatures. In this plot, one observes that Δ_C^2 is much larger than Δ_Q^2 in the whole temperature range under consid-

eration. This is not strange if one takes into account that the molecular rotation around the interstitial T site can be considered as a classical motion at these temperatures. In fact, the order of magnitude of this spatial delocalization can be obtained from the free motion of a particle on a spherical surface with radius equal to half distance between atoms in an H_2 molecule. For a distance $R=0.77$ Å, we obtain a mean-square classical displacement of 0.15 Å^2, close to the value of Δ_C^2 at 300 K. This magnitude increases for rising temperature, as expected for an increase in the fluctuations of the distance from each H atom to the average position (T site).

For the spreading of the quantum paths of each H atom we obtain at room temperature $\Delta_Q^2=0.03$ Å^2 and it decreases as temperature is raised. This gives for the paths an average extension of ~0.1 Å at 300 K, much smaller than the H–H distance, and thus justifying the neglect of quantum exchange between protons. Moreover, the fact that Δ_Q^2 is much smaller than Δ_C^2 in the temperature range considered here does not mean that quantum effects are irrelevant but is a consequence of the enhancement in Δ_C^2 due to molecular rotation.

D. Interatomic distance

As mentioned above, the interatomic distance between hydrogen atoms increases when the molecule is introduced from the gas phase into a silicon crystal due to the interaction between H and host atoms. For the minimum-energy distance we found $R_0=0.752$ Å, which is smaller that the values obtained in earlier calculations (0.788 Å in Ref. 14 and 0.817 Å in Refs. 11 and 47).

We now present the temperature dependence of the mean distance H–H for the three approaches considered above to study molecular hydrogen in silicon. Our results are displayed in Fig. 4, where symbols represent data points derived from PIMD simulations. For approach 1 (1d motion in a fixed lattice), we find at 300 K a mean distance $R=0.780$ Å, which represents an appreciable increase vs the distance obtained for the minimum-energy configuration. In this model, R increases very slowly as a function of T (squares in Fig. 4) since molecular rotation is not allowed and the molecule expansion is only due to the increasing population of excited vibrational levels. In fact, we find $dR/dT=1.0\times10^{-6}$ Å/K.

When molecular rotation is allowed in a fixed lattice (approach 2), we observe an increase in R (see circles in Fig. 4). At 300 K we found $R=0.785$ Å, about 5×10^{-3} Å larger than for 1d motion. Now R rises with temperature much faster than in approach 1 with $dR/dT=1.1\times10^{-5}$ Å/K. Next, we allow the Si atoms to move, introducing the full quantization of all degrees of freedom in the simulation cell, and we obtain a reduction in the distance H–H with respect to approach 2. This can be understood as due to a softening of the effective Si–H interaction, which decreases as a consequence of Si motion. In this case with full motion of the 66 atoms in the cell, we find $dR/dT=1.6\times10^{-5}$ Å/K, which means a larger slope than in approach 2.

It is interesting to compare these changes in the mean distance R with those corresponding to molecular hydrogen in the gas phase. To this end we have carried out some PIMD simulations of an isolated hydrogen molecule with the same interatomic potential. In this case we obtain an increase in R with temperature given by $dR/dT=7.5\times10^{-6}$ Å/K, a value clearly smaller than those obtained for H_2 in silicon in our approaches 2 and 3. This means that, for H_2 in silicon, the change in interatomic distance with temperature is controlled by both the centrifugal expansion due to rotation and interaction with the nearby host atoms.

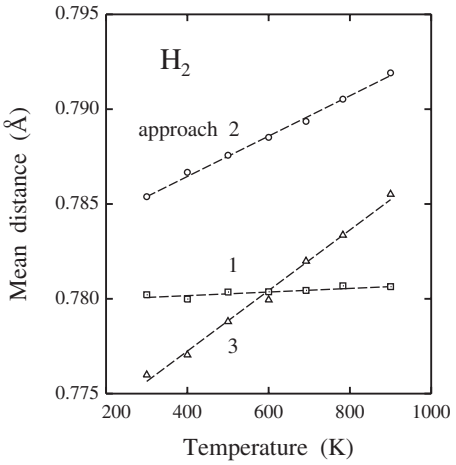

FIG. 4. Mean distance between H atoms in an H_2 molecule in silicon. Symbols correspond to different approximations for the molecular motion. Squares: motion of H_2 in one dimension with fixed host atoms (approach 1); circles: free motion of H_2 in a fixed silicon lattice (approach 2); triangles: free motion of H_2 and host atoms (approach 3). Error bars are in the order of the symbol size. Dashed lines are linear fits to the data points.

PIMD simulations can be also employed to study the isotopic dependence of the mean interatomic distance R. The molecular expansion with respect to the lowest-energy classical geometry is due to a combination of anharmonicity with quantum delocalization. One expects smaller distances for molecular deuterium due to its smaller vibrational amplitudes. In fact, at 300 K we found for D_2 in silicon, $R=0.767$ Å, to be compared with $R=0.776$ Å for H_2 at the same temperature and a distance $R_0=0.752$ Å for the lowest-energy position in the classical limit. In Fig. 5 we present the temperature dependence of the mean distance for both H_2 and D_2, as derived from our PIMD simulations for approach 3 (full motion of molecular hydrogen and host atoms). For D_2 we find $dR/dT=1.5(1)\times10^{-5}$ Å/K, which coincides within error bar with the slope obtained for H_2 in silicon in the temperature region from 300 to 900 K.

E. Stretching frequency

The stretching frequency of H_2 is an important fingerprint of the molecule, that in fact has been used to detect and characterize this impurity in the silicon bulk.[8,48] This stretching vibration has been found at 3618 cm^{-1} (at 4 K) independently by Raman[8] and infrared-absorption spectroscopies.[49]

In Fig. 6 we show the temperature dependence of ω_s for H_2 in the three approaches considered here, as derived from the LR method presented above. In approach 1 (1d motion)

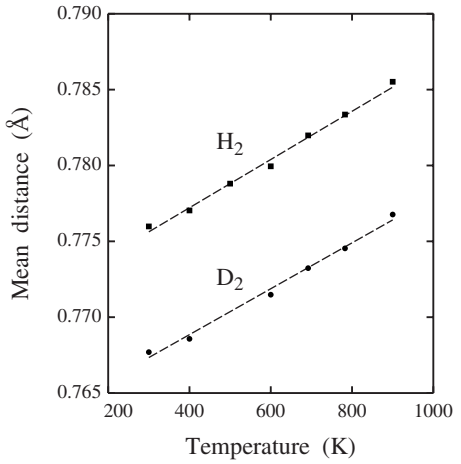

FIG. 5. Mean interatomic distance for H_2 and D_2 molecules in silicon, as a function of temperature. Symbols indicate results derived from PIMD simulations for approach 3, in which all atoms are mobile: squares for H_2 and circles for D_2. Error bars are on the order of the symbol size. Dashed lines are linear fits to the data points.

the frequency decreases slightly in the analyzed temperature range. In approaches 2 and 3, the coupling between molecular rotation and vibration causes an appreciable change in ω_s with the temperature. For model 2 (fixed Si lattice) we find $d\omega_s/dT=-0.13$ cm^{-1}/K, to be compared with a slope of $d\omega_s/dT=-0.24$ cm^{-1}/K for model 3, which includes motion of the host atoms. Thus, motion of the Si atoms causes a significant change in $d\omega_s/dT$, which becomes almost twice larger than in the case of a static Si lattice. It is interesting that at room temperature ω_s is smaller for model 2 than for approach 3 but due to its faster decrease in the latter approach, ω_s becomes smaller for model 3 at high T.

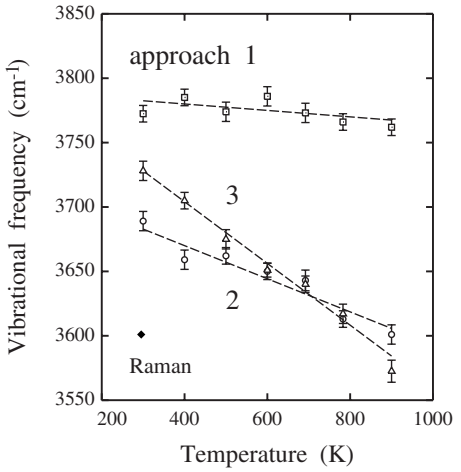

FIG. 6. Frequency of the stretching vibration of the H_2 molecule in silicon as a function of temperature. Symbols represent results derived from PIMD simulations in three different approximations: squares, motion of H_2 in one dimension in a fixed silicon lattice; circles, free motion of H_2 with fixed Si atoms; triangles, free motion of H_2, and Si atoms. Error bars correspond to the statistical uncertainty in the PIMD simulations. A black diamond indicates the stretching frequency obtained by Raman spectroscopy at room temperature (Ref. 8).

Something similar has been obtained for the stretching vibration of D_2. In particular, for approach 3 we find a rather constant ratio between the stretching frequencies of H_2 and D_2, that amounts to 1.37(1), somewhat smaller than the ratio expected in a harmonic approximation (1.41). Experimentally, a ratio of 1.37 is found from infrared[7] and Raman[8,44] spectra of H_2 and D_2 in silicon, a little smaller than the ratio 1.39 observed for these molecules in the gas phase.[50]

For the HD molecule in silicon, an infrared study allowed to determine the energy of the first excited rotational level.[45] In fact, a value of 73.9 cm^{-1} was found for the wave number difference between the levels $J=0$ and $J=1$, somewhat lower than that corresponding to the gas phase (89.3 cm^{-1}). By scaling that wave-number difference with the reduced mass, we expect for H_2 an energy difference of about 99 cm^{-1}. Since our PIMD simulations yield results for the average frequency ω_s, one can estimate a frequency shift from the rotational energy, taking into account the population and degeneracy of the different levels.[45] By considering only the levels $J=0$ and $J=1$, one would expect at room temperature a frequency shift $d\omega_s/dT$ on the order of -0.05 cm^{-1}/K, clearly lower than the value found from our simulations for approach 3 (-0.24 cm^{-1}/K). This is not strange, taking into account that at these temperatures higher rotational levels will be excited, contributing to a larger decrease in the average frequency. However, the actual position of these levels further than $J=1$ is not known at present and a more detailed comparison with our results is not possible.

We note that the quantum treatment of atomic nuclei in molecular-dynamics simulations is crucial to give a reliable description of the vibrational frequencies of light atoms, such as hydrogen. In fact, we have applied the LR method to calculate the stretching frequency ω_s from classical simulations. At 300 K we found for H_2 in silicon a frequency $\omega_s=4039$ cm^{-1} (for full motion of interstitial hydrogen and host atoms), to be compared with $\omega_s=3728$ cm^{-1} derived from PIMD simulations. As expected, the classical value is much closer to the frequency $\omega_s=4071$ cm^{-1} obtained in a HA for H_2 in silicon.

IV. DISCUSSION

In Sec. III we have presented results of our PIMD simulations for H_2 and D_2 in silicon. The main advantage of this kind of simulations is the possibility of calculating energies at finite temperatures, with the inclusion of quantization of host-atom motions, which are not easy to be accounted for in fixed-lattice calculations. Isotope effects can be readily explored since the impurity mass appears as a parameter in the calculations. This includes the consideration of zero-point motion, which together with anharmonicity gives rise to nontrivial effects. In addition, the vibrational motion of H_2 is coupled with molecular rotation, leading to a change in the stretching frequency with temperature.

As mentioned above, an important feature of isolated H_2 molecules in semiconductors is their stretching vibration ω_s. In a harmonic approximation, the tight-binding potential employed here yields for H_2 in silicon a frequency ω_s

$=4071\ \mathrm{cm}^{-1}$ vs $4397\ \mathrm{cm}^{-1}$ for H_2 in the gas phase, which means a reduction of about $330\ \mathrm{cm}^{-1}$ due to interaction with the host atoms. This reduction is accompanied by an increase in the H–H distance, as shown in Sec. III C. An additional decrease in ω_s is obtained when anharmonic effects are taken into account in a one-dimensional motion of the molecule in a fixed lattice. In fact, at 300 K the LR calculations give in this case $\omega_s=3770\ \mathrm{cm}^{-1}$, which means a decrease in frequency of about $300\ \mathrm{cm}^{-1}$ with respect to the HA for H_2 in silicon. This frequency change due to anharmonicity is in the order of that derived in Ref. 47 from DF calculations, namely, $\Delta\omega_s=-408\ \mathrm{cm}^{-1}$. This frequency is further lowered when full (quantum) motion of the molecule and host atoms are allowed, giving $\omega_s=3728\ \mathrm{cm}^{-1}$. In this latter reduction there is a contribution of two competing effects: coupling between molecular rotation and vibration, and interaction with Si atoms, whose motion allows for a larger delocalization of the H_2 molecule in the interstitial space.

In general we observe a correlation between ω_s and mean interatomic distance R in the H_2 molecule, in the sense that a rise in ω_s is accompanied by a decrease in R. This is in line with the general trend found by Van de Walle[11] for molecular hydrogen in crystalline semiconductors, as derived from DF calculations at $T=0$. However, this trend is not so strict when atomic motion is included at finite temperatures, as derived from Figs. 4 and 6. In this case, the mobile Si atoms may contribute to an additional decrease in the stretching frequency of H_2 by a rise in the effective mass associated to this vibrational mode.

In connection with this, it is clear that theoretical techniques to deal with the electronic structure of solids have been improving their precision over the years. For various purposes, the accuracy currently achieved by these methods is excellent, when comparing their predictions with experimental data. However, quantum-nuclear effects limit the accuracy of state-of-the-art techniques to predict actual properties of light impurities in solids. The answer to this question has to be found in *ab initio* path-integral simulations, where both electrons and nuclei are treated directly from first principles. But even in this case the question is not simple when one has to deal with phenomena such as molecular rotation at low temperatures, where a proper description of quantum rotation has to be included in the formalism.

There is an important challenging point that should be considered in future work. It refers to considering coupling between nuclear spins in the hydrogen molecule, i.e., dealing separately with ortho and para H_2 (both have been observed in silicon[12,44,51]). This becomes specially relevant at low temperatures, where the quantum character of molecular rotation has to be explicitly considered in the simulations. Usually these kind of calculations have been carried out by assuming the molecule to be a rigid rotor, without taking into account vibrations and deformations, and thus neglecting the rovibrational coupling.

An analysis of hydrogen diffusion in silicon is out of the scope of this paper. Actual diffusion coefficients are not directly accessible with the kind of simulations employed here since the time scale employed in the calculations is not readily connected to the real one. In this respect, PIMD simulations could be applied to study quantum diffusion of H_2 in silicon, by calculating free-energy barriers in a way similar to that employed earlier to study the diffusion of atomic hydrogen in metals[25] and semiconductors.[24,52]

In summary, the PIMD method has turned out to be well suited to study finite-temperature equilibrium properties of hydrogen molecules in silicon. This has allowed us to notice the importance of anharmonicity and rovibrational coupling in order to give a realistic description of the properties of these interstitial impurities. Anharmonicity shows up in the stretching motion of the molecules, causing important shifts with respect to the harmonic expectancy.

ACKNOWLEDGMENT

This work was supported by CICYT (Spain) through Grant No. BFM2006-12117-C04-03.

[1] S. J. Pearton, J. W. Corbett, and M. Stavola, *Hydrogen in Crystalline Semiconductors* (Springer, Berlin, 1992).
[2] S. K. Estreicher, Mater. Sci. Eng. R. **14**, 319 (1995).
[3] M. Stutzmann, J.-B. Chevrier, C. P. Herrero, and A. Breitschwerdt, Appl. Phys. A: Solids Surf. **53**, 47 (1991).
[4] A. Mainwood and A. M. Stoneham, Physica B (Amsterdam) **116**, 101 (1983).
[5] J. W. Corbett, S. N. Sahu, T. S. Shi, and L. C. Snyder, Phys. Lett. **93**A, 303 (1983).
[6] J. Vetterhöffer, J. Wagner, and J. Weber, Phys. Rev. Lett. **77**, 5409 (1996).
[7] R. E. Pritchard, M. J. Ashwin, J. H. Tucker, R. C. Newman, E. C. Lightowlers, M. J. Binns, S. A. McQuaid, and R. Falster, Phys. Rev. B **56**, 13118 (1997).
[8] A. W. R. Leitch, V. Alex, and J. Weber, Phys. Rev. Lett. **81**, 421 (1998).
[9] M. Hiller, E. V. Lavrov, J. Weber, B. Hourahine, R. Jones, and P. R. Briddon, Phys. Rev. B **72**, 153201 (2005).
[10] Y. Okamoto, M. Saito, and A. Oshiyama, Phys. Rev. B **56**, R10016 (1997).
[11] C. G. Van de Walle, Phys. Rev. Lett. **80**, 2177 (1998).
[12] E. E. Chen, M. Stavola, W. Beall Fowler, and J. A. Zhou, Phys. Rev. Lett. **88**, 245503 (2002).
[13] Y. Okamoto, M. Saito, and A. Oshiyama, Phys. Rev. B **58**, 7701 (1998).
[14] B. Hourahine, R. Jones, S. Öberg, R. C. Newman, P. R. Briddon, and E. Roduner, Phys. Rev. B **57**, R12666 (1998).
[15] J. M. Pruneda, S. K. Estreicher, J. Junquera, J. Ferrer, and P. Ordejón, Phys. Rev. B **65**, 075210 (2002).
[16] W. B. Fowler, P. Walters, and M. Stavola, Phys. Rev. B **66**, 075216 (2002).
[17] B. Hourahine and R. Jones, Phys. Rev. B **67**, 121205(R) (2003).
[18] M. J. Gillan, Philos. Mag. A **58**, 257 (1988).
[19] D. M. Ceperley, Rev. Mod. Phys. **67**, 279 (1995).

[20] R. Ramírez and C. P. Herrero, Phys. Rev. Lett. **73**, 126 (1994).
[21] C. P. Herrero and R. Ramírez, Phys. Rev. B **51**, 16761 (1995).
[22] T. Miyake, T. Ogitsu, and S. Tsuneyuki, Phys. Rev. Lett. **81**, 1873 (1998).
[23] C. P. Herrero, R. Ramírez, and E. R. Hernández, Phys. Rev. B **73**, 245211 (2006).
[24] C. P. Herrero and R. Ramírez, Phys. Rev. Lett. **99**, 205504 (2007).
[25] T. R. Mattsson and G. Wahnström, Phys. Rev. B **51**, 1885 (1995).
[26] C. P. Herrero and R. Ramírez, Phys. Rev. B **79**, 115429 (2009).
[27] M. C. Gordillo, J. Boronat, and J. Casulleras, Phys. Rev. B **65**, 014503 (2001).
[28] E. Kaxiras and Z. Guo, Phys. Rev. B **49**, 11822 (1994).
[29] M. P. Surh, K. J. Runge, T. W. Barbee, E. L. Pollock, and C. Mailhiot, Phys. Rev. B **55**, 11330 (1997).
[30] C. Chakravarty, Phys. Rev. B **59**, 3590 (1999).
[31] H. Kitamura, S. Tsuneyuki, T. Ogitsu, and T. Miyake, Nature (London) **404**, 259 (2000).
[32] R. P. Feynman, *Statistical Mechanics* (Addison-Wesley, New York, 1972).
[33] H. Kleinert, *Path Integrals in Quantum Mechanics, Statistics and Polymer Physics* (World Scientific, Singapore, 1990).
[34] G. J. Martyna, M. E. Tuckerman, D. J. Tobias, and M. L. Klein, Mol. Phys. **87**, 1117 (1996).
[35] M. E. Tuckerman, in *Quantum Simulations of Complex Many-Body Systems: From Theory to Algorithms*, edited by J. Grotendorst, D. Marx, and A. Muramatsu (NIC, FZ Jülich, 2002), p. 269.
[36] D. Porezag, T. Frauenheim, T. Köhler, G. Seifert, and R. Kaschner, Phys. Rev. B **51**, 12947 (1995).
[37] R. Ramírez and T. López-Ciudad, J. Chem. Phys. **115**, 103 (2001).
[38] C. M. Goringe, D. R. Bowler, and E. Hernández, Rep. Prog. Phys. **60**, 1447 (1997).
[39] R. Ramírez and M. C. Böhm, Int. J. Quantum Chem. **34**, 571 (1988).
[40] M. E. Tuckerman and A. Hughes, in *Classical and Quantum Dynamics in Condensed Phase Simulations*, edited by B. J. Berne, G. Ciccotti, and D. F. Coker (Word Scientific, Singapore, 1998), p. 311.
[41] R. Ramírez and T. López-Ciudad, in *Quantum Simulations of Complex Many-Body Systems: From Theory to Algorithms*, edited by J. Grotendorst, D. Marx, and A. Muramatsu (NIC, FZ Jülich, 2002), pp. 325–375; for downloads and audio-visual lecture notes see www.theochem.rub.de/go/cprev.html.
[42] T. López-Ciudad, R. Ramírez, J. Schulte, and M. C. Böhm, J. Chem. Phys. **119**, 4328 (2003).
[43] R. Ramírez and C. P. Herrero, Phys. Rev. B **72**, 024303 (2005).
[44] E. V. Lavrov and J. Weber, Phys. Rev. Lett. **89**, 215501 (2002).
[45] E. E. Chen, M. Stavola, W. B. Fowler, and P. Walters, Phys. Rev. Lett. **88**, 105507 (2002).
[46] M. F. Herman, E. J. Bruskin, and B. J. Berne, J. Chem. Phys. **76**, 5150 (1982).
[47] C. G. Van de Walle and J. P. Goss, Mater. Sci. Eng., B **58**, 17 (1999).
[48] J. A. Zhou and M. Stavola, Phys. Rev. Lett. **83**, 1351 (1999).
[49] R. E. Pritchard, M. J. Ashwin, J. H. Tucker, and R. C. Newman, Phys. Rev. B **57**, R15048 (1998).
[50] B. P. Stoicheff, Can. J. Phys. **35**, 730 (1957).
[51] M. Hiller, E. V. Lavrov, and J. Weber, Phys. Rev. Lett. **98**, 055504 (2007).
[52] C. P. Herrero, Phys. Rev. B **55**, 9235 (1997).